Control of Cu Microstructure and Properties for Low-Temperature Direct Cu-Cu Bonding

Cara Gannett[1], Youngmin Yoon[1], Gabrielle Page[1], Derek Thoresen[1], Brian Parquette[2], Matthew Gole[1], Matthew Van Hanehem[3], Ravi Pokhrel[1]
DuPont
[1]Marlborough, MA 01752 USA
[2]Wilmington, DE 19805 USA
[3]Newark, DE 19713 USA
Ph: 508-481-7950
Email: cara.gannett@dupont.com

Abstract

3D heterogeneous integration offers significant improvements in terms of input/output density, faster processing speeds, and reduced power consumption. Cu-Cu hybrid bonding is critical for unlocking the full potential of this technology. However, high temperatures associated with the Cu-Cu bonding process have limited the scope of this technology. Two primary strategies have been proposed for modifying Cu microstructure to enable low-temperature bonding capabilities: (111)-oriented, nanotwinned Cu and fine-grained Cu. Herein, we demonstrate the ability to reliably deposit both types of Cu microstructures on blanket and patterned segments by modifying bath additives and plating conditions. To be viable for high-volume manufacturing, functional Cu deposits must be stable for several weeks and persist through the processing steps prior to bonding. In this study, we investigate the stability of Cu deposits with time and through the chemical mechanical polishing (CMP) process. We report the Cu microstructure before and after CMP by x-ray diffraction (XRD), focused ion beam scanning electron microscopy (FIB-SEM), and electron backscattered diffraction (EBSD) analysis. Further, we seek to understand the unique properties of fine-grained Cu that determine its stability under various annealing conditions. To this end, we perform experiments to quantify stress in the deposits, characterize grain boundaries, and measure dopant levels. By understanding the properties associated with Cu grain stability, we can improve our formulations for features with decreasing and mixed critical dimensions associated with next-generation hybrid bonding.

Key words

Cu microstructure, electrodeposition, heterogeneous integration, direct Cu-Cu bonding.

I. Introduction

Heterogeneous integration schemes have been proposed as a possible solution to lead the semiconductor chips industry into the "more than Moore" era. 3D packaging will be key to enabling these schemes and the resultant improvement in the performance, speed, and bandwidth of future advanced devices. 3D packaging requires the development of advanced wafer and die bonding processes to stack die efficiently and reliably. Further, to fully realize the benefits of 3D integration, the pitch associated with the interconnects within these must be reduced to very small dimensions, 10 µm and below. Historically, solder microbumps have been used to stack die; however, reduction of pitch dimensions below 10 µm creates several challenges for solder technology. Instead, direct Cu-Cu bonding is widely proposed to replace solder joints in this space. This approach offers several benefits over solder, including improving interconnect electrical conductivity, preventing solder bridging at dense pitches, and eliminating the formation of intermetallic compounds (IMC)[1],[2].

While direct Cu-Cu bonding offers clear advantages, traditional direct bonding of Cu requires high temperatures to achieve Cu diffusion across the bonding interface. Unfortunately, these high temperatures are incompatible with temperature-sensitive components such as DRAM and can lead to substrate warpage. To overcome these limitations and extend the application space of direct Cu-Cu bonding, methods have been developed to reduce the temperature associated with bond formation. One popular approach is to

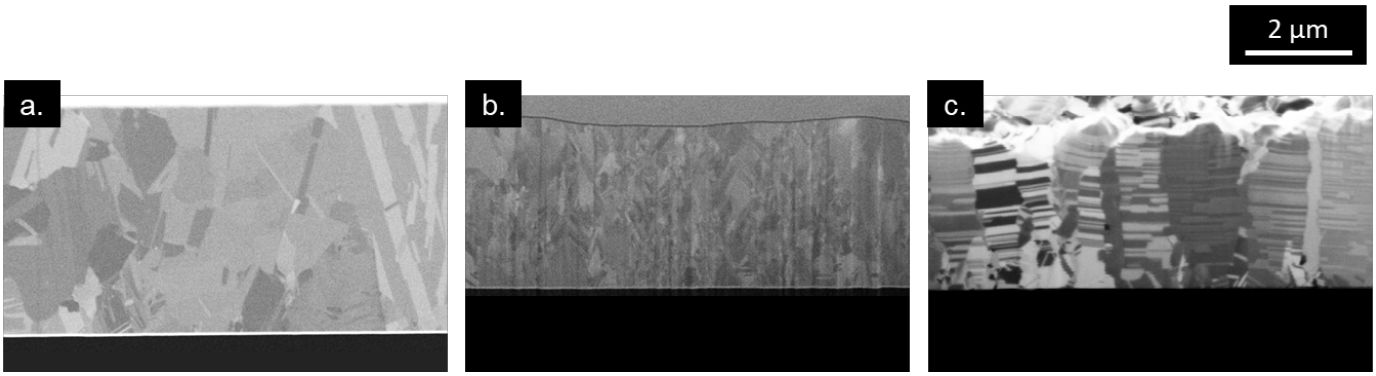

Fig. 1 FIB-SEM images of a) Coarse grain Cu (CG), b) Fine-grain Cu (FG), and c) (111)-oriented, nanotwinned Cu ((111)Cu).

modify the Cu electroplating bath to yield Cu deposits with improved Cu diffusion across the bonding interface. Two widely pursued methods for achieving this are (111)-oriented, nanotwinned Cu and fine-grained copper deposits [3]-[6].

Herein, we demonstrate our ability to electrodeposit stable (111)-oriented and fine-grain Cu on blanket wafers by modifying our plating bath chemistry. We explore their stability at room temperature, during chemical mechanical polishing (CMP), and under annealing conditions relevant to low-temperature Cu-Cu bonding applications. Further, we probe some of the properties we believe play influential roles in determining the room temperature stability of our fine grain formulation including dopant concentration, stress, and microstrain.

II. Results and Discussion

A. Experimental

Coupons were cut into ~ 4 cm x 4 cm segments from a 300 mm Si wafer with a 40 nm Ti and 150 nm Cu seed layer. Coupons were mounted to segment holders and plated in a custom plating tool with agitation from both rotation of the wafer segment and pump driven solution flow parallel to the wafer segment. The plating bath was one compartment (no membrane) and used a soluble Cu anode. The base electroplating solution explored in this work was made up of copper sulfate, sulfuric acid, and hydrochloric acid. The microstructure of the Cu was controlled by the incorporation of commercial and experimental additives from DuPont.

Grain size of bulk deposits was evaluated by x-ray diffraction (XRD). The XRD patterns were fit using the HighScore software package from Malvern Panalytical to determine crystallite size, peak intensity area, and % microstrain. The N_{avg} crystallite size for a sample was calculated by using a weighted average of the crystallite size of the (111), (200), (220), and (311) facets which accounted for peak intensities normalized to their relative scattering intensities.

Stress was measured using a Bruker ContourX-200 Optical Profilometer to measure the warpage across a wafer segment before and after a Cu film was deposited in the center. The warpage after Cu deposition was measured at the unplated edges. The radius of curvature and the Stoney equation were used to compute stress [7].

Cu resistivity was measured using a Filmetrics R50 contact four-point probe. The thickness of the sample was measured by x-ray fluorescence and used to calculate resistivity.

B. Demonstration of Cu Microstructure

By modifying the additives in our plating baths, we can change the microstructure of our Cu deposits, as shown in **Fig. 1**. Specifically, we have demonstrated the ability to produce coarse-grained Cu (CG), fine-grained Cu (FG), and (111)-oriented, nanotwinned Cu deposits ((111)Cu). Notably, our CG deposits exhibit an initial small-grain size, followed by grain growth over the course of ~24 hours, as measured by XRD (**Fig. 2**). In contrast, our FG formulation demonstrates significantly improved stability, showing an average grain growth of only ~10 nm over a period of 2+ months. We observe the (111)Cu deposit exhibits relatively little grain growth. We expect this could arise from several effects. (111)-oriented Cu often exhibits a high density of twin boundaries which reduced the energy of the deposit [6],[8]. Further, the initial grain size of (111)Cu is

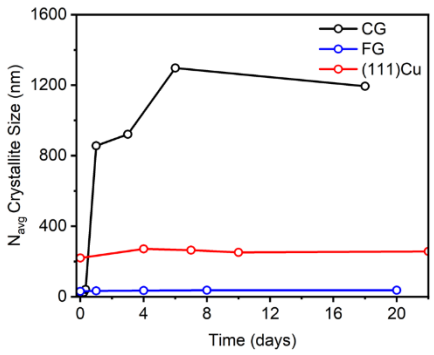

Fig. 2 Grain size from XRD patterns of CG, FG, and (111)Cu samples left to rest at room temperature. When not being analyzed, the samples were stored in a N_2 box.

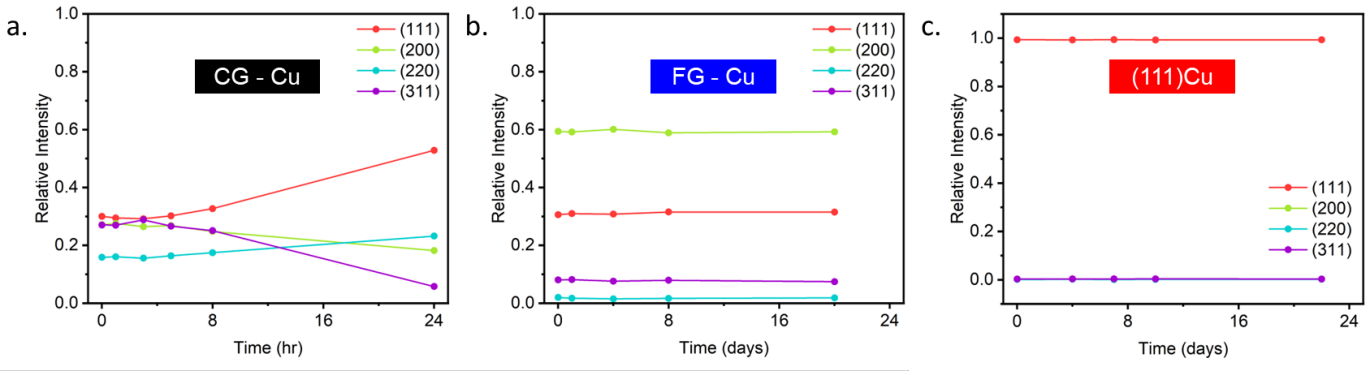

Fig. 3 Relative intensity of Cu diffraction peaks with self-annealing for a) CG, b) FG, and c) (111)Cu. Peak areas have been normalized to the relative scattering intensities of respective Cu facets.

significantly larger and would have fewer grain boundaries amounting to a lower grain boundary energy and a reduced driving force for grain growth [9].

We also compared the relative orientations of the different Cu formulations through XRD analysis. The areas of the (111), (200), (220), and (311) peaks have been normalized to their x-ray scattering intensities and the relative values are plotted in **Fig. 3**. As expected, the (111)Cu shows a strong (111) preference, with negligible peak areas from the other Cu facets. Interestingly, CG also exhibits a slight preference towards the (111) orientation, although initially the Cu is plated without a preferred orientation. As the sample anneals at room temperature, the (111) peak intensity and grain size grows, implying that much of the grain growth this driven by the growth of the (111)-oriented grains in the sample. Interestingly, the FG sample exhibits a preference for a (200) orientation. For Cu, the (111) crystallographic orientation is generally the preferred orientation for Cu electrodeposition because it possesses the lowest surface energy [10]. Meanwhile, the (200) texture is known to have a reduced strain energy [11]. The authors hypothesize that a higher density of (200)-oriented crystallites may reduce the strain in the sample and be responsible, in part, for the improved stability of the fine grains in this sample.

To gain further insight into the orientation at the surface of the Cu deposit (instead of the orientation of the bulk deposit, as reflected in the XRD analysis), we analyzed the exposed surface of our Cu after CMP by electron backscatter diffraction (EBSD). The top-down orientation mapping image (**Fig. 4a**) reflects the surface that would act as the bonding interface for direct Cu-Cu bonding. Here, we observed an extremely high ratio of (111)-oriented Cu – 97.3% of the surface was found to be (111)-oriented Cu, allowing for a maximum deviation of 15°. EBSD mapping of a cross section of the sample demonstrates the (111)-orientation extends through the deposit (**Fig. 4b**). However, it is worth noting that when this formulation was deposited in small via features (2 – 10 µm in diameter), we observed a decrease in (111)-orientation at the top surface as feature size decreased. This effect was attributed to the electrodeposition of (111)-oriented Cu on the side walls of the via in addition to the bottom surface and has been previously noted in other work [12].

To achieve void-free joints during Cu-Cu direct bonding, it is essential to start with very flat and debris-free Cu

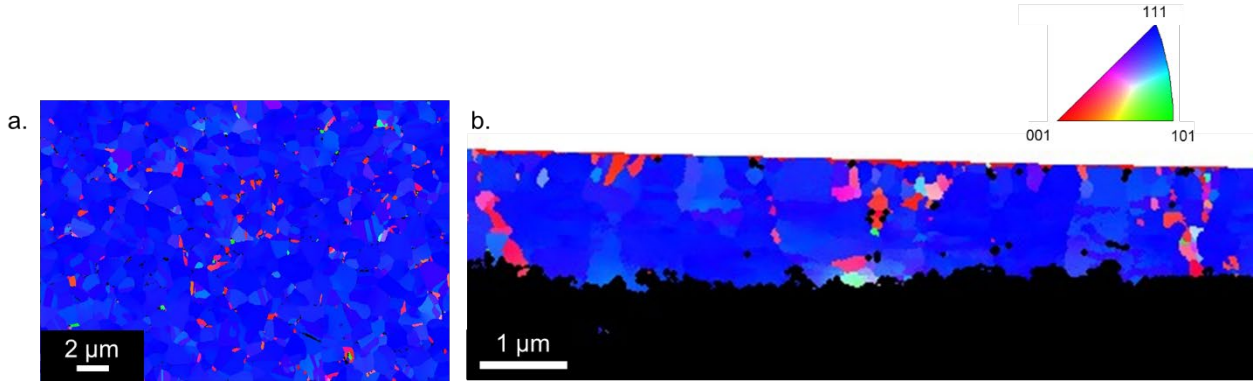

Fig. 4 EBSD image of the crystallographic mapping of a (111)Cu sample plated on a blanket wafer after CMP, a) top-down view, b) cross-sectional image (top of figure is Si wafer on which the Cu has been electrodeposited).

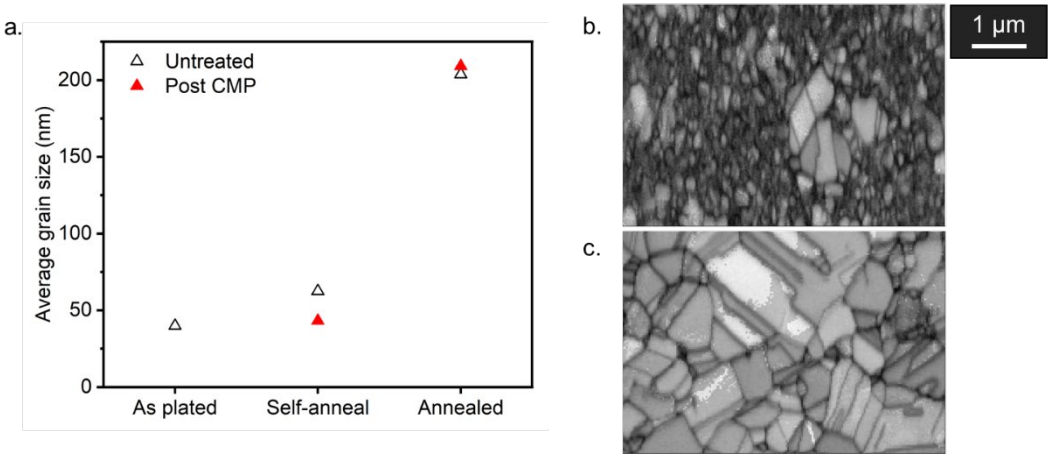

Fig. 5 a) Grain size from XRD of two sets of FG samples plated in the same bath. One set of samples underwent CMP (red triangles), while the other served as a control to monitor grain size in the absence of CMP (black, open triangles). Both samples exhibited similar grain size after self-annealing for 2 months and after annealing for 90 s at 225 °C. EBSD band contrast images of FG that had undergone CMP and b) self-annealed, or c) was annealed at 225 °C.

surfaces. Therefore, it is crucial that our Cu formulations are compatible with the CMP process. All the Cu formulations reported here were subjected to CMP and demonstrated compatibility with reasonable clear times. Additionally, it is imperative for the microstructure at the surface to be retained after CMP to ensure the application's success. To verify that the FG formulation could maintain its microstructure after CMP, we analyzed the grain size by both XRD and EBSD (**Fig. 5**). We observed no significant changes in the bulk Cu grain size after CMP using XRD analysis. Furthermore, the fine grain size at the exposed surface was largely retained after CMP, as shown by EBSD analysis. Notably, the EBSD image was acquired 4 months after plating our Cu sample, further demonstrating the room temperature stability of the FG deposit.

In addition to demonstrating the stability of our Cu deposits, it is also critical to report on their high-temperature behavior as a proxy for microstructure evolution during the bonding process. The CG sample did not exhibit significant changes in grain size with annealing, suggesting that the grains had self-annealed to nearly their maximum size (as shown in **Fig. 6a**). On the other hand, the FG formulation exhibited a dramatic thermal response, growing almost 30X its size with annealing, with the extent of growth being both temperature and time-dependent.

We observed that some fine grain formulations (an example being FG-B) do not exhibit nearly as significant growth at elevated temperatures. By SIMS analysis, we found that these samples had high dopant concentrations (as shown in **Table I.**). We believe that the dopants pin the grains in these samples and limit grain growth at both room and elevated temperatures. This is a distinguishing feature of the FG formulation presented in this work – its low dopant concentration enables it to anneal at elevated temperatures yet maintain grain stability at room temperature and through CMP processing steps. Further, FIB-SEM images reveal that samples with higher doping form voids in the Cu when annealed (**Fig. 6b** and **c**). The low dopant concentration associated with the FG formulation leads to grain coarsening with no visible voids after annealing. Meanwhile, FG-B has visibly less regular grain growth across the sample and several voids appear after annealing, likely from the migration and coalesce of dopants in the sample [13].

Aside from limiting grain growth, we also observed that the dopants affected the resistivity of the deposit (**Table I.**). Specifically, the highly doped, FG-B formulation exhibited an increased resistivity compared to the higher purity deposits. Unsurprisingly, we found that the resistivity was higher in samples with small grain size (CG and FG before annealing), but this resistivity decreased and approached the theoretical value for Cu (1.77 µΩ-cm) as the grain size increased with annealing. We observed that the (111)Cu sample had initially lower resistivity than the Cu deposits with smaller grain sizes, but this resistivity did not change significantly with annealing. We hypothesize that this is due to the higher dopant concentration in the sample relative to the CG and FG formulations.

We wanted to better understand the properties of FG which enable its unique room temperature grain stability. We compared the stress in our formulations and found CG is initially deposited under compressive stress. As the sample anneals at room temperature, the compressive stress decreases (**Fig. 7a**). We expect that the grain boundaries in the sample impose a biaxial stress on the Cu which is

Table I. Dopant concentrations from SIMS analysis and resistivity values from four-point probe analysis.

Formulation	Dopant concentration (ppm/wCu)	ρ (µΩ-cm) As plated	ρ (µΩ-cm) After Anneal
CG	9	2.2 ± 0.02	1.85 ± 0.03
FG	13-31	2.2 ± 0.1	1.85 ± 0.07
FG-B	795	2.27 ± 0.05	2.23 ± 0.12
(111)Cu	89	2.02 ± 0.02	2.07 ± 0.13

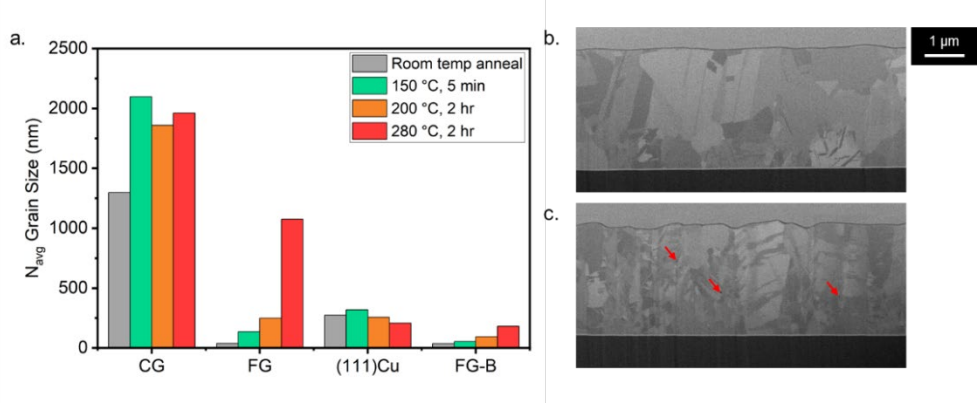

Fig. 7 a) Grain size from XRD fitting for annealed Cu samples. FIB SEM images of annealed samples of b) FG and c) FG-B. The red arrows in c) are used to indicate voids observed in the sample after annealing.

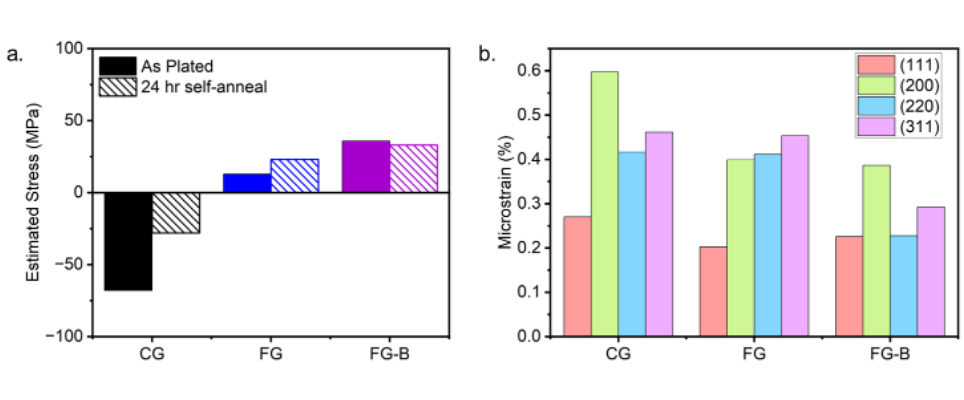

Fig. 6 a) Stress values from warpage measurements. b) Microstrain from XRD fits.

partially alleviated as the density of grains boundaries decreases with grain growth. This may, in part, explain the propensity for CG to spontaneously anneal at room temperature.[11,14] Meanwhile, both the fine grain Cu samples (FG and FG-B) exhibit tensile stress, notably lower in magnitude than CG, as plated. As the sample is left to rest at room temperature for 24 hours, we observe minor changes in the stress — an increase for FG and decrease for FG-B. We hypothesize that the reduced stress and the nature of the stress (tensile) do not provide the same driving force for self-annealing in the fine grain Cu samples.

We further explored this phenomenon using strain measurements obtained from fitting our XRD patterns. Based on the Lorentzian nature of the Cu diffraction peaks, the percent microstrain (% strain) of the Cu film can be calculated. We found that CG exhibits a relatively high initial % strain in the (200) peak. Meanwhile, our fine grain Cu formulations have lower % strain in all Cu peaks. We find this trend holds true across a wide range of samples with slightly modified formulations/concentrations of additives – when all crystallites exhibit % strain values below ~ 0.5%, the grains exhibit room temperature stability. When one of the crystallographic peaks exhibits strain values above this threshold, the sample spontaneously anneals at room temperature. We hypothesize that this strain could be related to the number of crystallographic defects in the Cu. A higher defect energy in a sample could accelerate recrystallization.[10,15] We expect the defect density/%strain in our fine grain sample sits below some critical threshold where the strain in the Cu drives spontaneous self-annealing properties.

III. Conclusion

Herein, we have demonstrated the ability to control Cu microstructure by changing our Cu electroplating bath formulations. We reported a highly (111)-oriented Cu on blanket coupons that demonstrates CMP compatibility. Further, we show a fine grain Cu chemistry which retains small grain size at room temperature over 4 months and grows 30x its initial size when annealed at 280 °C. This Cu is also stable during CMP, exhibits low doping concentration, and low resistivity after annealing. Finally, we compare the stress and strain in this deposit relative to a formulation which spontaneously anneals at room temperature and find both are lower for our fine grain formulation. We hypothesize that the lower stress in our Cu deposit reduces the driving force for self-annealing below some threshold value such that we can retain grain size in our Cu deposits until the thermal anneal step. We expect these properties will be especially beneficial for direct Cu-Cu bonding.

References

[1] H. Ren, Y. T. Yang, S. S. Iyer, "Recess effect study and process optimization of sub-10 μm pitch die-to-wafer hybrid bonding" , IEEE 72nd Electronic Components and Technology Conference, 2022, pp. 149–156, DOI: 10.1109/ECTC51906.2022.00034.

[2] M. Murugensan, K. Mori, M. Sawa, E. Sone, M. Koyanagi, T. Fukushima, "Cu–SiO_2 hybrid bonding yield enhancement through Cu grain enlargement", IEEE 72nd Electronic Components and Technology Conference, 2022, pp. 685-690, DOI: 10.1109/ECTC51906.2022.00115.

[3] C. M. Liu, H. W. Lin, Y. S. Huang, Y. C. Chu, C. Chen, D. R. Lyu, K. N. Chen, K. N. Tu, "Low-temperature direct copper-to-copper bonding enabled by creep on (111) surfaces of nanotwinned Cu", Sci. Rep., vol. 5 (2015) pp. 1–11, DOI: 10.1038/srep09734.

[4] L. Mirkarimi, C. Uzoh, D. Suwito, B. Lee, G. Fountain, T. Workman, J. Theil, G. Gao, B. Buckalew, J. Oberst, T. Ponnuswamy, " The influence of Cu microstructure on thermal budget in hybrid bonding", IEEE 72nd Electronic Components and Technology Conference, 2022, pp. 162–167 DOI: 10.1109/ECTC51906.2022.00036.

[5] W. L. Chiu, O. H. Lee, C. W. Chiang, H. H. Chang, "Low-Temperature wafer-to-wafer hybrid bonding by nanocrystalline copper", IEEE 72nd Electronic Components and Technology Conference, 2022, pp. 679–684, DOI: 10.1109/ECTC51906.2022.00114.

[6] B. Rebhan, K. Hingerl, "Physical mechanisms of copper-copper wafer bonding", *J. Appl. Phy.,* vol. 118, no. 13 (2015) pp. 135301, DOI: 10.1063/1.4932146.

[7] S. Timoshenko, "Analysis of bi-metal thermostats", *J. Opt. Soc. Am*., vol. 11, no. 3 (1925) pp. 233-255, DOI: 10.1364/JOSA.11.000233.

[8] G. Gottstein, *Physikalische Grundlagen der Materialkunde*. Berlin Heidelberg: SpringerVerlag, 2007, pp. 83–100.

[9] R. N. Stevens, "Grain boundary sliding and diffusion creep", *Surface Science*, vol. 31 (1972*)* pp.543-565, DOI: 10.1016/0039-6028(72)90274-9.

[10] M. Stangl, M. Lipták, A. Fletcher, J. Acker, J. Thomas, H. Wendrock, S. Oswald, K. Wetzig. "Influence of initial microstructure and impurities on Cu room-temperature recrystallization (self-annealing)", *Microelectronic Engineering,* vol.85, no. 3 (2008) pp. 534-541, DOI: 10.1016/j.mee.2007.09.007.

[11] V. A. Vas' Ko, I. Tabakovic, S. C. Riemer, M. T. Kief, "Effect of organic additives on structure, resistivity, and room-temperature recrystallization of electrodeposited copper", *Microelectronic engineering*, vol. 75, no. 1 (2004) pp. 71-77, DOI: 10.1016/j.mee.2003.10.008.

[12] S. Yang, D. Tran, J. Ong, W. Chiu, H. Chang, C. Chen, "Periodic reverse electrodeposition of (1 1 1)-oriented nanotwinned Cu in small damascene SiO2 vias", *J. Electroanalytical Chem.*, vol. 935 (2023) pp. 117328. DOI: 10.1016/j.jelechem.2023.117328.

[13] J. Wang, J. Chen, L. Zhang, Z. Zhang, Y. Han, X. Hu, H. Lu, S. Zhang, 2022. "Forming mechanism and growth of Kirkendall voids of Sn/Cu joints for electronic packaging: A recent review," *Journal of Advanced Joining Processes*, vol. 6 (2022) pp.100125, DOI: 10.1016/j.jajp.2022.100125.

[14] R. Huang, W. Robl, H. Ceric, T. Detzel, G. Dehm, "Stress, sheet resistance, and microstructure evolution of electroplated Cu films during self-annealing", *IEEE Transactions on Device and Materials Reliability,* vol. 10, no. 1 (2009) pp. 47-54, DOI: 10.1109/TDMR.2009.2032768.

[15] R. Koch, "The intrinsic stress of polycrystalline and epitaxial thin metal films", *J. Phys. Condens. Matter*, vol. 6 (1994) pp. 9519-9550, DOI: 10.1088/0953-8984/6/45/005.